

I give permission for public access to my thesis and for copying to be done at the discretion of the archives' librarian and/or the College library.

Gracia Cheng

4/30/2020

Signature

Date

Genetic Analysis of Tissue Remodeling and Lipid Storage in *Drosophila*

melanogaster

by

Gracia Cheng (Xinran Cheng)

A Paper Presented to the

Faculty of Mount Holyoke College in

Partial Fulfillment of the Requirements for

the Degree of Bachelors of Arts with

Honor

Program in Biochemistry

South Hadley, MA 01075

This paper was prepared
under the direction of
Professor Craig Woodard
for eight credits.

ACKNOWLEDGMENTS

I want to say thank you to my project advisor Professor Craig Woodard for his help and support during my research, to Microscopy Director Sarah Kiemle for teaching me and supporting my project, to the MHC Program in Biochemistry for funding, to other members of Woodard Lab for being lovely teammates, and finally to all fruit flies that were sacrificed purposely or accidentally in my research.

TABLE OF CONTENTS

| | Page |
|-----------------------------|------|
| LIST OF FIGURES | v |
| ABSTRACT | vii |
| INTRODUCTION | 1 |
| MATERIALS AND METHODS | 13 |
| RESULTS | 17 |
| DISCUSSION | 38 |
| LITERATURE CITED | 44 |

LIST OF FIGURES

| | Page |
|-----------------|--------|
| Figure 1 | 4 |
| Figure 2 | 6 |
| Figure 3 | 9 |
| Figure 4 | 10 |
| Figure 5 | 11 |
| Figure 6 | 18 |
| Figure 7 | 19 |
| Figure 8 | 20 |
| Figure 9 | 21 |
| Figure 10 | 23 |
| Figure 11 | 24 |
| Figure 12 | 25 |
| Figure 13 | 27 |
| Figure 14 | 29 |
| Figure 15 | 30 |
| Figure 16 | 31 |
| Figure 17 | 33 |
| Figure 18 | 35 |
| Figure 19 | 36, 37 |

Figure 20 41

ABSTRACT

Tissue remodeling has been used as a model to study cancer. It is also an important process during the development of *Drosophila melanogaster*. During *D. melanogaster* metamorphosis, which is the transition from the larva stage to the adult stage, larval fat body remodeling occurs. The larval fat body changes from a single-cell layered sheet of connected cells to individual sphere-like motile cells that supply energy to the organism. Failed or abnormal fat body remodeling can result in death during the pupal stage.

In my research, I examined the abnormal larval fat body remodeling phenotype in three *D. melanogaster* mutant lines. All three lines were incompletely penetrant for the abnormal larval fat body remodeling phenotype. I also observed possible developmental delay in mutant lines during the head eversion process. In addition, I noticed that there are two types of remodeled larval fat bodies - whitish fat bodies and clear fat bodies in both wild type and in the mutant lines. I stained remodeled larval fat bodies to detect lipid droplets and nuclei under fluorescence. Further research should continue on staining of identified whitish and clear fat bodies to visualize lipid storage, which might give insights into the regulation of nutrient during metamorphosis.

INTRODUCTION

Tissue remodeling

Tissue remodeling is the process of reorganizing existing tissues, often involving connective protein degradation. During remodeling, in order to allow for reorganization, the connective proteins in cell-cell junctions and the basement membrane are cleaved by enzymes called matrix metalloproteinases (MMPs). MMPs are specific to different types of connective proteins (Tiede et al., 2016), and mutations in genes encoding MMPs could lead to serious problems in development.

Tissue remodeling plays a key role in health and diseases, including cancer therapy, development disorders, wound healing, and tumor metastasis (Lu et al., 2011). It is found in various species and cell types. During wound healing, the extracellular matrix (ECM) degrades in order to remove damaged cells, and failure of this process could lead to defects such as tissue fibrosis and cancers (Lu et al., 2011). Tumor cell-mediated ECM remodeling could promote tumor cell metastasis (Oudin et al., 2016), and remodeling of tumor cells allow them to travel to a different site (Cox & Erler, 2011). Given the similarities between the synthesis of proteolytic components during non-neoplastic tissue remodeling and the interaction between tumor cells and stromal cells during cancer invasion, tissue remodeling could be used as a model of

studying extracellular proteolysis happening in cancer (Johnsen et al., 1998). Studying of the interplay between stromal cells and tumor cells during cancer invasion might lead to significant progress in cancer mechanism and cancer therapy. It has been stated that cancer invasion could be considered uncontrollable tissue remodeling. (DANØ et al., 1999).

Tissue remodeling is an important process during the development of *Drosophila melanogaster*. It allows successful metamorphosis to happen, in which a larva transforms into an adult fly. Thus, studying how tissue remodeling happens and how it is regulated during *D. melanogaster* development could lead to a better understanding of tissue remodeling in human physiology and diseases such as cancer.

Drosophila melanogaster

Drosophila melanogaster, the fruit fly, is a popular model organism used in genetic studies. Its advantages include a short life cycle that allows for fast reproduction, ease of culture, and various phenotypes that allow for observation of mutations. In addition, the *D. melanogaster* genome has similarities with the human genome, and its biological pathways are conserved with vertebrates. One example of tissue remodeling is the remodeling of larval fat bodies during metamorphosis

in *D. melanogaster*. This process makes *D. melanogaster* a good model organism for the study of tissue remodeling (Jennings 2011).

The *Drosophila* life cycle.

The life cycle of *D. melanogaster* includes four major stages: embryo, larva, pupa and adult (Figure 1). The larval stage has three minor stages: the 1st, 2nd and 3rd instars (Weigmann et al., 2003).

The whole life cycle takes about 14 days, while it takes about 5-8 days to arrive at the prepupal stage - the starting point of metamorphosis. During the first two instars, the larva stays in the food, and its main goal is to eat and store enough energy for later metamorphosis. After the expected energy storage has been reached, the 3rd instar larva leaves the food and gets prepared for the prepupa stage, which takes ~12-24 hours. When the larva is well-prepared, the puparium (the pupal case), which is white and soft, will form, marking the beginning of the prepupal stage. The larva also gets shorter and becomes motionless. This time point is also called zero hours after puparium formation (0h APF).

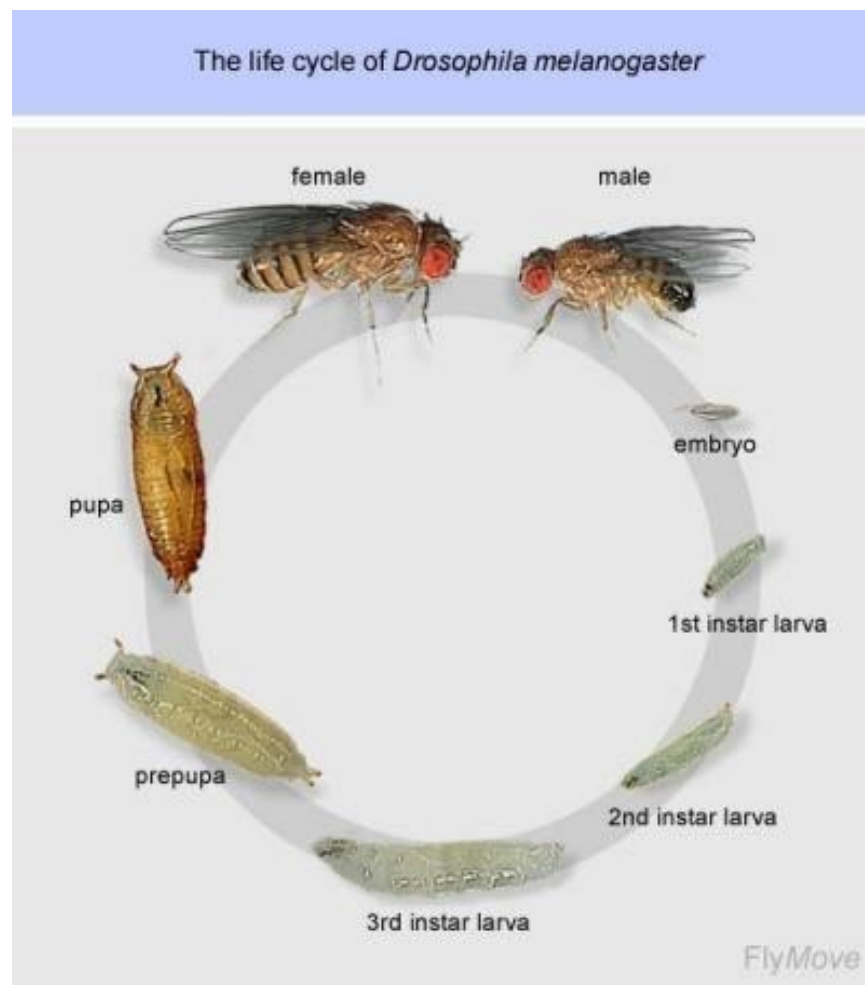


Figure 1. The life cycle of *Drosophila melanogaster*. Starting as an embryo, an individual undergoes the 1st, 2nd, and 3rd instars to form the prepupa. The prepupa starts metamorphosis, changes into a pupa and becomes an adult fly. The whole process from an embryo to an adult fly could take on to two weeks (Weigmann et al., 2003).

Later, the puparium becomes hard and yellowish-brown. At about 12h APF, the transition from the prepupal stage to the pupal stage happens, and this is when the majority of larval fat body remodeling (FBR) occurs. Metamorphosis lasts about 6 days, after which the adult fly will emerge from the puparium. During metamorphosis, most of larval tissues undergo destruction via programmed cell death and are

replaced by adult tissues, while the larval fat body remodels and the cells are retained until a few days after the adult stage begins (Riddiford & Truman 1993; Tyler 2000; Weigmann et al. 2003).

Drosophila larval fat bodies

Fat bodies play an important role in that they are responsible for providing energy for metamorphosis, since the pupa cannot move around and feed itself. The fat body cells are in clusters before the prepupal stage, forming single-cell layered sheets, and during remodeling, at about 6 hours APF, they start becoming individual sphere-like motile cells (Figure 2) (Franz et al., 2018). This change allows them to move around the organism and provide energy for the process happening simultaneously at different regions. Failure or abnormality in the fat body remodeling could result in pharate adult (PA) lethality during the pupa stage, which is death due to the inability to enclose after metamorphosis has completed. The mechanism of how incomplete fat body remodeling leads to PA lethality is still unclear (Nelliot et al., 2006).

As major components of metabolism in *D. melanogaster*, fat bodies are mainly made up of lipids, glycogen, and proteins. Lipid droplet is the major form of lipid storage, and lipid storage droplet proteins (Lsds) and lipases are

necessary to regulate lipid metabolism. Two types of Lsds, Lsd1 and Lsd2, are expressed in *D. melanogaster*, where Lsd1 promotes lipolysis and Lsd2 stimulates lipogenesis. Types of lipases promoting lipolysis include Brummer, hormone-sensitive lipase (HSL), and acid lipase (Li et al., 2019).

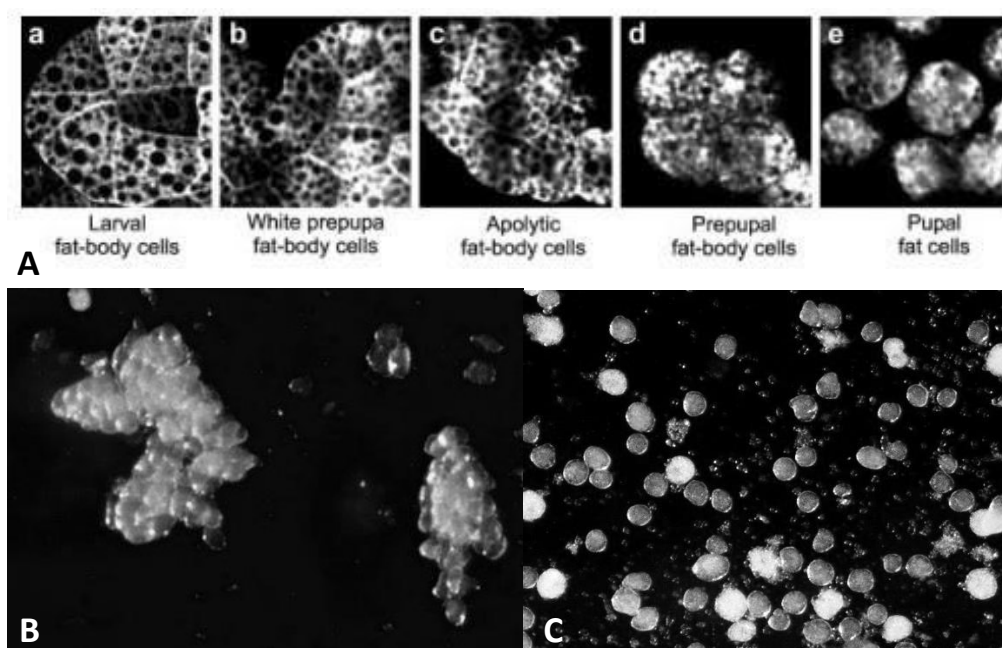


Figure 2. (A) The change in larval fat bodies during prepupa-pupa transition. The cell-shape changes from flat, sheet-like larval fat cells to spherical cells that are disassociated from each other. Images taken by a confocal microscope at the stage of (a) third-instar larva; (b) white prepupa; (c) apolytic animal; (d) prepupa; and (e) early-stage pupa (Nelliot et al., 2006). (B) An example of fat bodies in chunks of single-cell layered sheets. Image taken by Gracia and edited with Photoshop. (C) An example of remodeled individual sphere-like fat bodies. Image taken by Gracia and edited with Photoshop.

Regulation of *Drosophila* metamorphosis

The steroid hormone 20-hydroxyecdysone (ecdysone) is a key hormone that regulates the larval-to-adult process. Pulses of ecdysone signal important steps during the development, which includes the larva-prepupal transition and prepupal-pupal transition. Ecdysone signaling promotes the programmed cell-death of old larval tissues and the formation of new adult organs (Thummel, 1996), while, as mentioned in the previous section, larval fat bodies are reserved during metamorphosis. The expression of two matrix metalloproteinases (MMPs), MMP1 and MMP2, are necessary in this process: MMP1 mainly digests the cell-cell junctions, while MMP2 mainly digests the basement membrane. Two MMPs together enable the separation of connected fat bodies to free fat bodies (Jia et al., 2014). Recent research has identified nuclear hormone receptor β *FTZ-F1* as the key gene to be induced punctually at the transcriptional level by ecdysone during prepupa-pupa transition at 10-12h APF (Bond et al., 2011; Ruaud et al., 2010).

Genetic mutation of abnormal FBR lines

In the Woodard Lab's previous studies, some abnormal fat-body-remodeling (FBR) lines of *D. melanogaster* had been mapped with a single mutation on the third chromosome that led to PA lethality.

One of those lines, *l(3)LL-15241* (15241) had been identified as partially FBR and PA lethality (Iqbal, 2018). It was examined in my research as one of the three mutant lines.

Aurora A (Aur-A) participates in the process of cytoskeletal arrangement during mitosis, which involves both actin microfilaments and microtubules. Overexpression of Aur-A could lead to cytokinesis failures (Moon & Matsuzaki, 2013). *Aur-A*¹⁴⁶⁴¹ had been mapped as partially FBR and PA lethality (Gausz et al., 1981). *Aur-A*⁸⁸³⁹, with a different mutation on the same gene, had been observed to be PA lethal and hypothesized to have abnormal FBR phenotype.

The *TM6B, Hu Tb* balancer chromosome is marked with the dominant, *Tubby* (Tb) mutation. Prepupae and pupae carrying *TM6B, Hu Tb* display the *Tubby* phenotype (shorter and fatter than wild type). Thus, as an example, *aur-A*¹⁴⁶⁴¹/*TM6B, Hu Tb* prepupae and pupae, which will be *Tubby*, can be distinguished from *aur-A*¹⁴⁶⁴¹ homozygotes, which will not be *Tubby* (of normal length) (Figure 3). It allows easy sorting of the mutant homozygotes, which are the individuals of interest. In addition, since *aur-A*¹⁴⁶⁴¹ homozygotes can't reproduce, heterozygotes with *Tubby* maintain the fly stock through reproduction of more homozygotes. Wild type used as controls in this research included the CS (Canton-Special)

and w^{1118} . The CS was used as a control to access the abnormal FBR features of mutant lines, while w^{1118} were used for staining remodeled fat bodies.

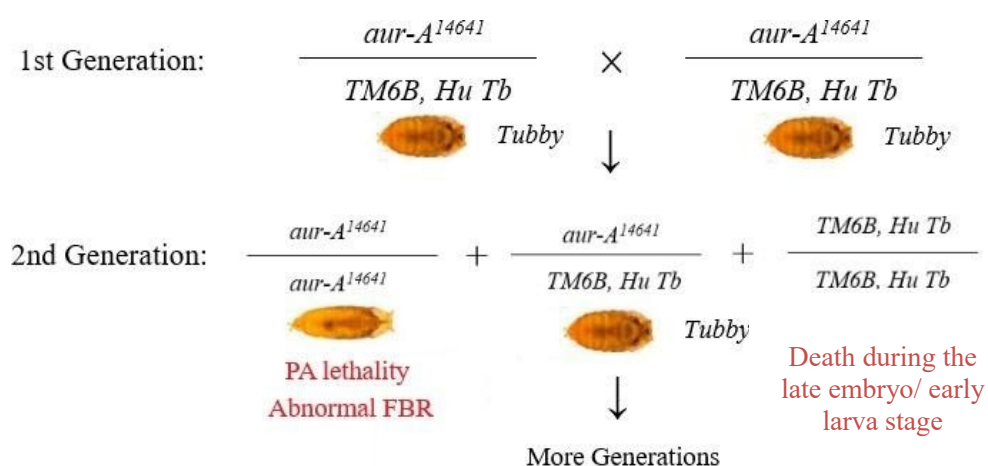


Figure 3. A diagram showing the reproduction method of an abnormal FBR mutant line, taking $aur-A^{14641}/TM6B, Hu Tb$ as an example. Prepupae and pupae carrying $TM6B, Hu Tb$, which is dominant, display the Tubby phenotype (shorter and fatter than wild type). Thus, only $aur-A^{14641}$ homozygotes are of normal length. They cannot reproduce new generations because of the PA lethality feature, and they are the mutant individuals of interest, hypothesized to have the abnormal FBR phenotype. Images of pupae from Chyb & Gompel, 2013.

Confocal microscopy and staining of *Drosophila* fat bodies

Invented by Marvin Minsky in 1955, confocal microscopy allows us to remove most of the light that is not from the microscope's focal plane. It generates sharp images of a sample that will blur under a conventional microscope (Figure 4). It is also able to reduce haze, improve contrast and present a thin cross-section (one focal plane) of a sample (Semwogerere & Weeks, 2005).

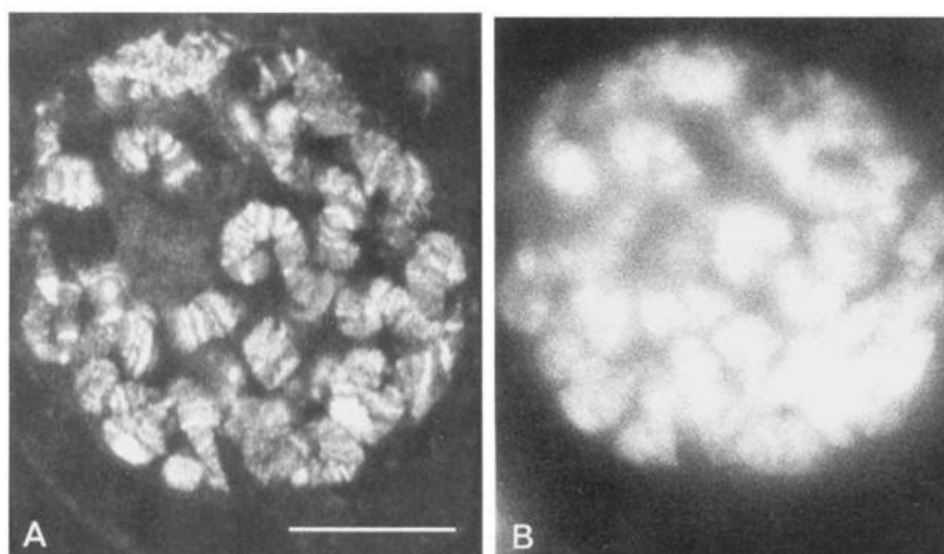


Figure 4. Images of nuclei in preparations of salivary glands of *Drosophila* larvae, chromosomes stained with chromomycin A3. A was created by a confocal microscope, and B was created by a conventional microscope on similar scale. The confocal image is sharper and contains more details of the chromosomal structure (White et al., 1987).

Nile Red (9-diethylamino-5-benzo [a] phenoxazinone), is a highly specific vital stain that acts like a near-ideal lysochrome, and it allows the detection of intracellular lipid droplets by fluorescence microscopy. It can be used for cells in an aqueous medium and will not dissolve the lipids (Greenspan et al., 1985). Compared to other lipid droplet stains like Oil Red O dye, it is more conducive and time efficient. It has been used to stain *Drosophila* fat bodies in previous studies including Grönke et al., 2003 and Okamura et al., 2007.

To present a better image of the fat body structure, DAPI (4',6-diamidino-2-phenylindole), a DNA-specific fluorescent probe, has been used as an addition to Nile Red lipid droplets stain. It

attaches to the minor groove of A-T rich sequences of DNA to form a fluorescent complex (Kapuscinski, 1995). In Kamoshida et al., 2012, Nile Red and DAPI were used to stain 3rd instar larval fat bodies (Figure 5).

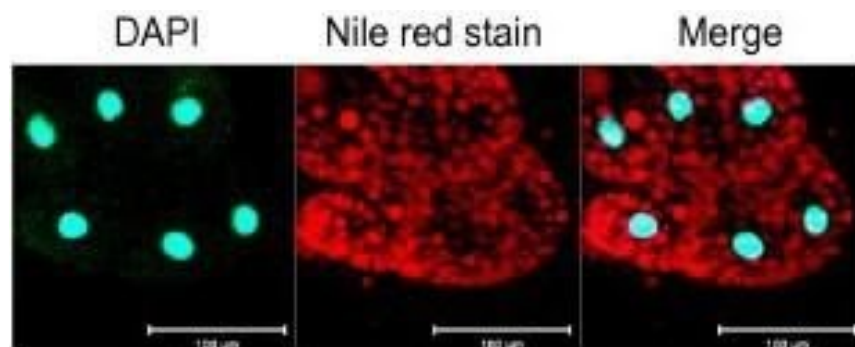


Figure 5. Nile Red and DAPI staining of fat bodies during 3rd instar larval stage. The bar marks 100 µm. The left image shows nucleus stained by DAPI under fluorescence (green). The middle image shows lipid droplets stained by Nile Red under fluorescence (red). The right image shows stained nucleus and stained lipid droplets together (Kamoshida et al., 2012).

Goals and Hypothesis

In my research, I examined the abnormal FBR feature of three *D. melanogaster* mutant lines, *aur-A*¹⁴⁶⁴¹, *aur-A*⁸⁸³⁹, and *l(3)LL-15241* (15241) by dissection during metamorphosis. They were predicted to show either complete or partially deficiency in fat body remodeling behavior compared to wild type. I also recorded some features of *Drosophila* fat bodies observed during multiple dissections on mutant and control lines, which included 1) possible developmental delay during the head eversion process on three mutant lines, and 2) the common existence of whitish and clear fat bodies in

both mutant and control individuals. To further explore possible reasons causing the two types of fat bodies, I **stained remodeled larval fat bodies of wild type w^{1118} with Nile Red on lipid droplets and DAPI on nucleus.** The fluorescence was examined by a confocal microscope. My larger goal was to provide data on how genetic mutations caused failures in tissue remodeling and their influence on *Drosophila* development, which might lead to important results in research on cancer mechanism and therapy.

MATERIALS AND METHODS

Drosophila Culturing

The fly stocks were kept at 25 °C in either vials or bottles. They were transferred to new vials or bottles one to three times per week, depending on their speed of growth and reproduction. They were fed with the Nutri-Fly Bloomington Formulation fly food. Yeast was added to vials and bottles before transferring of flies to aid their reproduction.

Preparation

Non-*Tubby* prepupae with normal length at 0 hour APF were selected for dissection from mutant lines. They should have their pupal cases formed and are still white. Aged prepupae were kept in petri dishes on damp filter papers without visible spray. The filter papers were made wet by distilled water. Different lines were kept in separate dishes and with the time point of 0 hour APF labeled. Petri dishes were kept in a plastic container with damp paper towels inside, without visible spray. The container was kept at 25 °C until the prepupae got dissected at 10-16 hours APF.

Dissection and Imaging

Pupae from mutant lines (*aur-A*¹⁴⁶⁴¹, *aur-A*⁸⁸³⁹, and 15241) with the control lines (CS and *w*¹¹¹⁸) were dissected 10-16 hours APF in 1X phosphate buffered saline (PBS) on a depression slide under a Nikon SMZ1500

stereomicroscope. Images were taken by a SPOT Insight QE camera linked to SPOT Imaging Solutions 5.0 software. For each pupa, an image was taken before dissection to identify its stage of development. Then, tweezers were used to hold the pupa's anterior and posterior. The pupal case was expected to be removed without damaging the pupa inside, but sometimes I had them taken apart at the same time. After the pupal case was removed, images were taken with various magnifications. Any large section of the pupa's body would be carefully broken apart. Both the overall view of the dissected pupa and closed images of fat bodies were taken. The images were named by the mutant line and the individual's age. Images were adjusted for brightness and contrast by Adobe Photoshop CS6. Colors were removed in all figures used in this thesis to eliminate the effect of light colors.

Lipid Droplets Staining and Imaging

The buffer solution was prepared with of PBS (pH 7.2) with 1% BSA, stored at 4 °C. An imaging spacer was attached to a slide to create a well. 3-7 pupae of the same genotype were dissected in buffer solution on the slide, according to the steps described above. All other organs were removed except for the larval fat bodies. Under the stereoscope, the buffer was removed and 200 μ L of 0.2% Tritan was added, which acted as a detergent to break the cell walls. After 5min incubation at room temperature, the 0.2% Tritan was removed, and the sample was washed with the buffer for three times. 200 μ L

of 4% paraformaldehyde was added, which fixed the cells. After 10 min incubation at room temperature, the 4% paraformaldehyde was removed, and the sample was washed with the buffer for three times. 200 μ L of the buffer was added, and the sample was incubated for 60 min at room temperature, the 1% BSA in the buffer reduced non-specific binding between the dye and the sample. More buffer solution could be added during the incubation to prevent the sample from drying out.

The Nile Red Staining Solution was prepared with 2 μ L Nile Red in 1 mL buffer solution, stored at -20 °C. Under the stereoscope, the buffer was removed as much as possible. 200 μ L of the Nile Red Staining Solution was added, and the sample was incubated for 30 min at room temperature in the dark. Under the stereoscope, the Nile Red Staining Solution was removed as much as possible. 2 μ L lipid mounting solution (with DAPI) was added, and the buffer solution was added to fill up the imaging spacer without creating a convex surface. The top layer of the imaging spacer was removed to expose the glue. A coverslip was added slowly with a tweezers. The slide was incubated in the dark for 20-24 hours to cure. The labeled fat bodies were imaged with a Nikon Motorized Eclipse Ti2 inverted laser scanning confocal microscope. I used the 30x or 40x objectives and 405-nm and 561-nm lasers controlled by NIS Elements software. Z series were collected with a 200 nm step size with the 40x objective and reassembled in the software. The

Maximum Z-projection images are highlighted in the result section. The fat body nuclei were labeled with the DAPI and excited with 405-nm laser and the lipid droplets were labeled with Nile Red and excited with 561-nm laser.

RESULTS

Abnormal FBR feature of *aur-A*¹⁴⁶⁴¹

At 12h APF, the majority of larval fat bodies were individual sphere-like cells, while a few clusters were observed. There was no significant difference observed in the degree of remodeling between the mutant line and wild type (Figure 6).

At 14h APF, both large clusters of larval fat bodies and individual fat bodies were observed. There was no significant difference observed in the degree of remodeling between the mutant line and wild type. More individual fat bodies were observed in the CS than in *aur-A*¹⁴⁶⁴¹ (Figure 7).

At 12h APF, the majority of larval fat bodies were individual sphere-like cells, while tiny clusters were observed. There was no significant difference observed in the degree of remodeling between the mutant line and wild type. More individual fat bodies were observed in the CS than in *aur-A*¹⁴⁶⁴¹ (Figure 8).

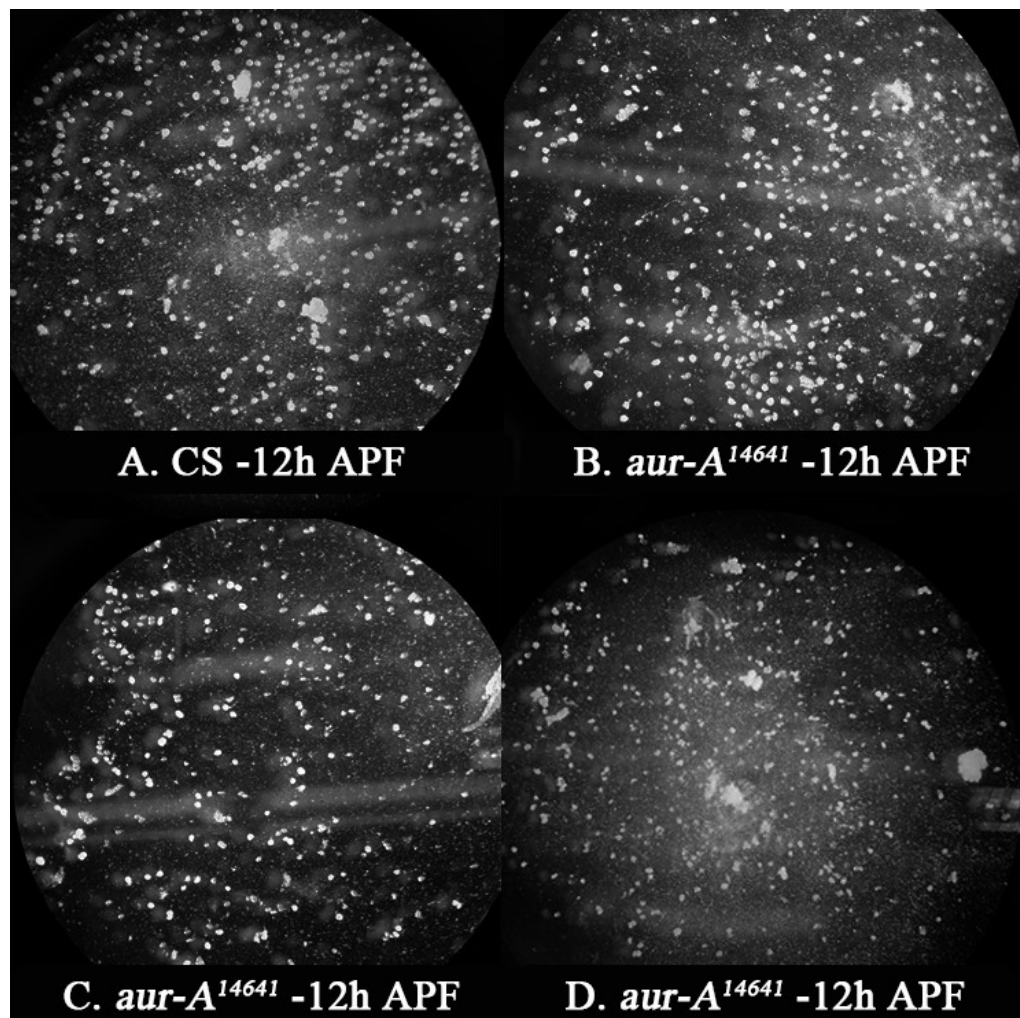


Figure 6. Fat body remodeling of mutant samples compared to wild type at 12h APF. A shows the fat body remodeling of the CS while B and C show the fat body remodeling of *aur-A*¹⁴⁶⁴¹. Images taken with my smartphone through the dissecting microscope and edited by Photoshop.

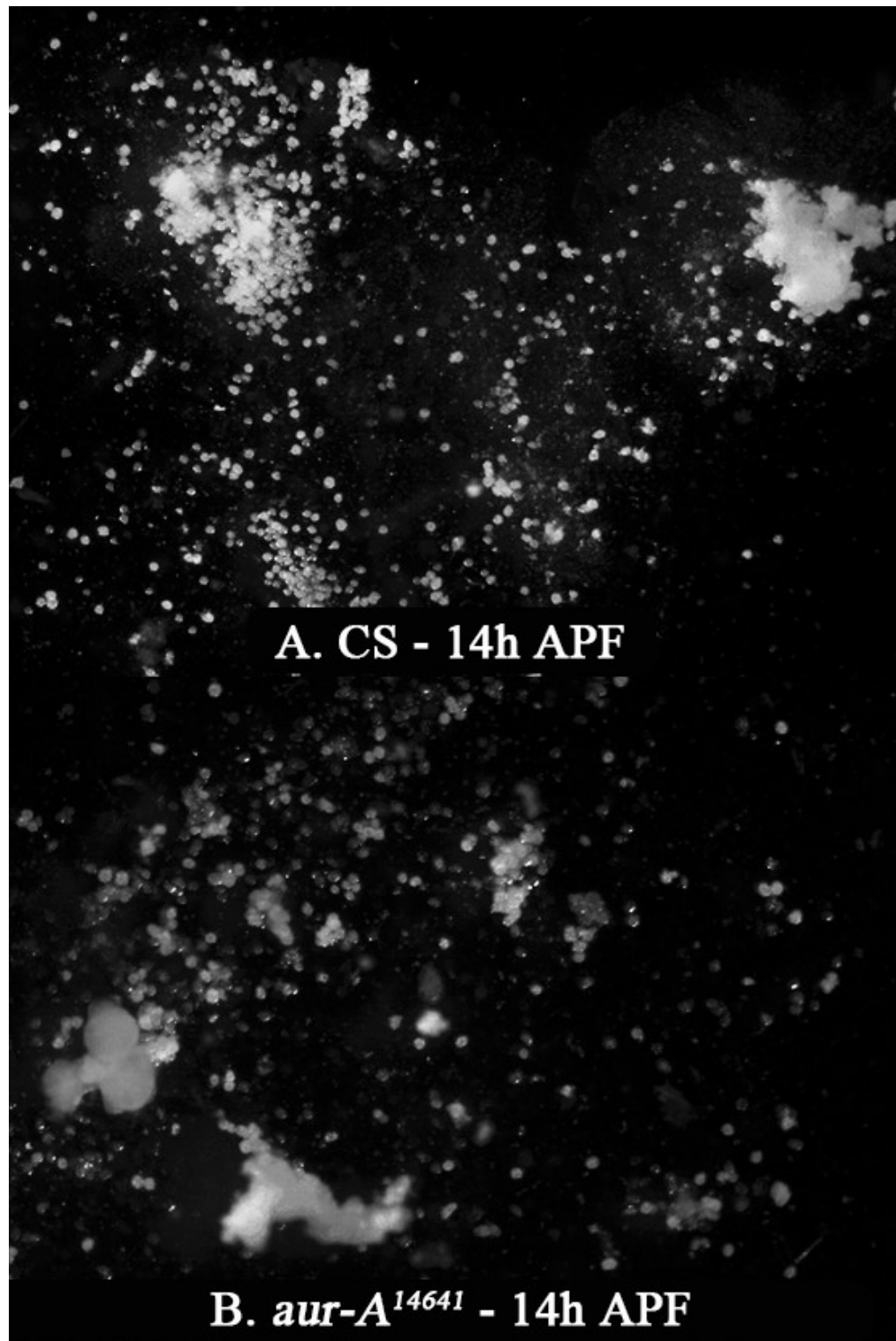


Figure 7. Fat body remodeling of mutant samples compared to wild type at 14h APF. A shows the fat body remodeling of the CS while B shows the fat body remodeling of *aur-A*¹⁴⁶⁴¹. Images taken with the stereoscope and edited by Photoshop.

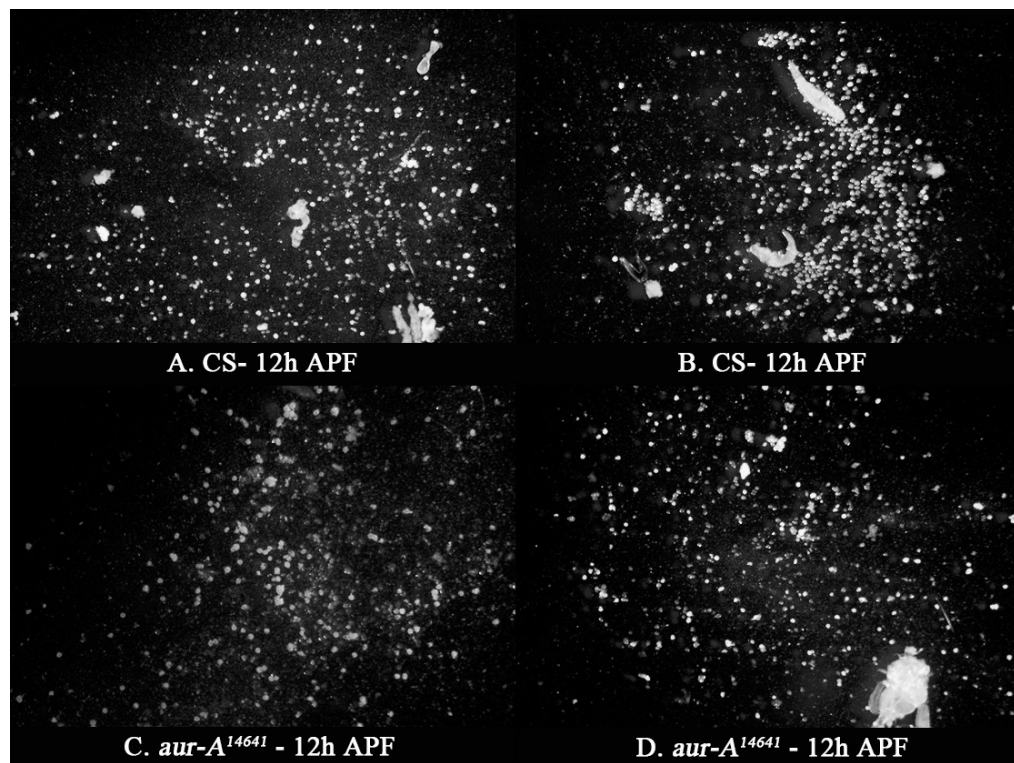


Figure 8. Fat body remodeling of mutant samples compared to wild type at 12h APF. A and B show the fat body remodeling of the CS while C and D show the fat body remodeling of *aur-A*¹⁴⁶⁴¹. Images taken with the stereoscope and edited by Photoshop.

Possible developmental delay during metamorphosis was observed in most samples of *aur-A*¹⁴⁶⁴¹ at both 12h APF and 14h APF during dissection. The gas bubble, which is related to the process of head eversion during metamorphosis, should move from the posterior to the anterior in order to make space for the adult head (Robertson 1936). At both 12h APF and 14h APF, the CS had their bubbles at the anterior end, while the mutant line still had their bubbles in the middle. In addition, the shapes of the CS pupae were transformed to the adult stage further than the mutant lines (Figure 9).

Not all samples imaged were included in this paper for *aur-A*¹⁴⁶⁴¹.

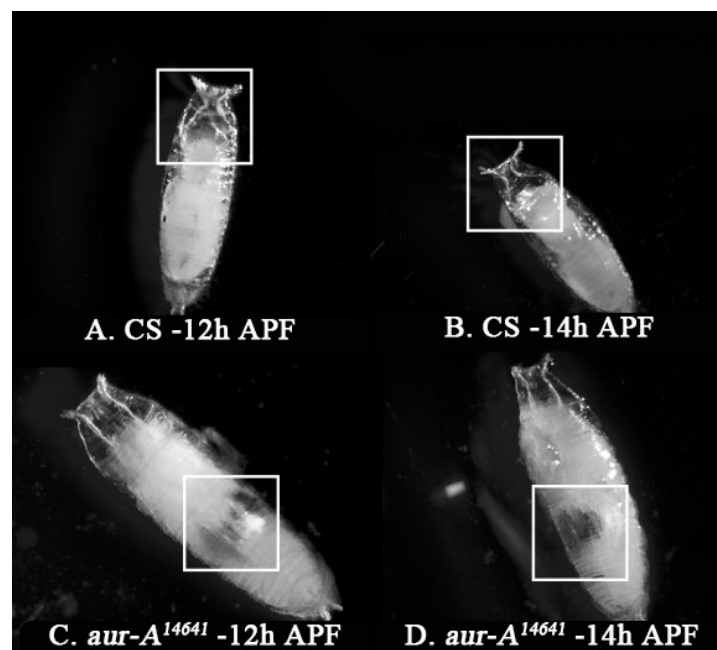


Figure 9. Possible developmental delay was observed at 12h APF (C) and 14h APF (D) in the mutant line *aur-A*¹⁴⁶⁴¹ compared to wild type (A, B). Images taken with the stereoscope and edited by Photoshop.

Abnormal FBR feature of *aur-A*⁸⁸³⁹

At 14h APF, the majority of larval fat bodies were individual sphere-like cells (Figure 10). Tiny clusters of fat bodies were observed in the second sample (Figure 10-B). There was no significant difference observed in the degree of remodeling between the mutant line and wild type (Figure 7-A). More individual fat bodies were observed in the CS than *aur-A*⁸⁸³⁹ (Figure 10).

At 11h APF, the majority of larval fat bodies were individual sphere-like cells (Figure 11). Some clusters of fat bodies were observed in both samples. There was no significant difference observed in the degree of remodeling between the mutant line and wild type. More individual fat bodies were observed in the *aur-A*⁸⁸³⁹ than the CS (Figure 11).

At 12h APF, the majority of larval fat bodies were individual sphere-like cells (Figure 12). Some clusters of fat bodies were observed in both samples. There was no significant difference observed in the degree of remodeling between the mutant line and wild type (Figure 12).

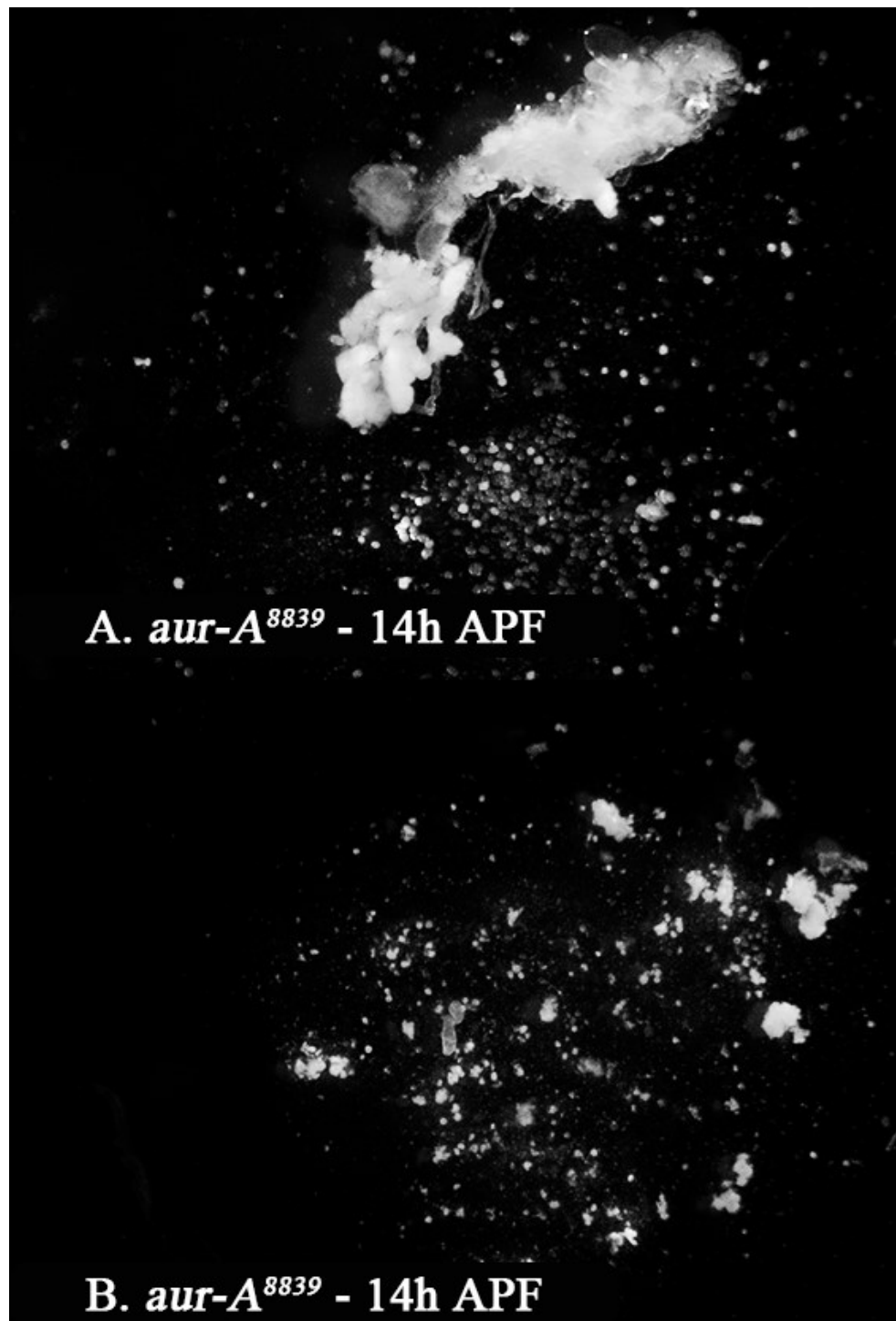


Figure 10. Fat body remodeling of mutant samples at 14h APF. A and B show the fat body remodeling of *aur-A*⁸⁸³⁹. Images taken with the stereoscope and edited by Photoshop.

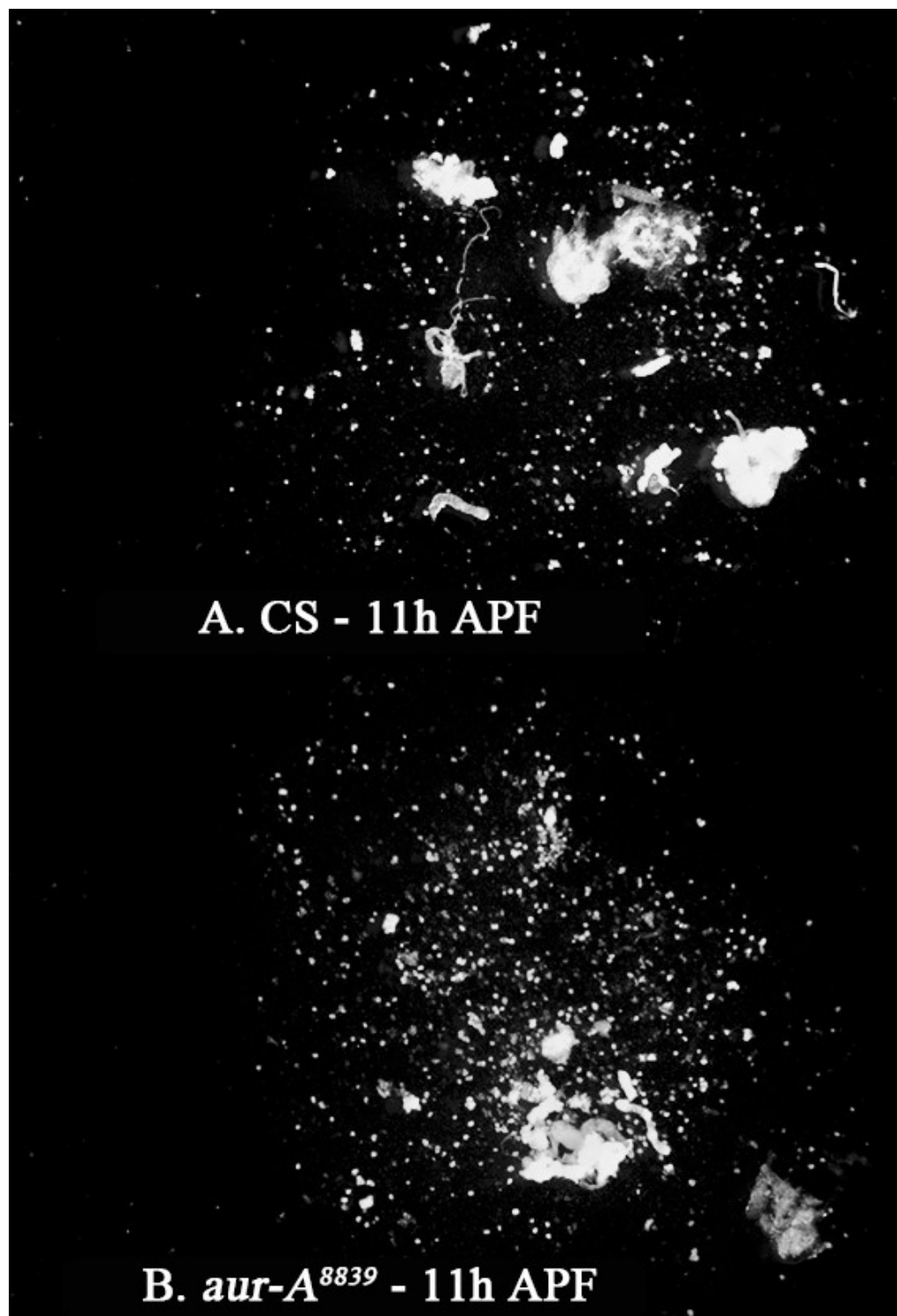


Figure 11. Fat body remodeling of mutant samples compared to wild type at 11h APF. A shows the fat body remodeling of the CS while B shows the fat body remodeling of *aur-A*⁸⁸³⁹. Images taken with the stereoscope and edited by Photoshop.

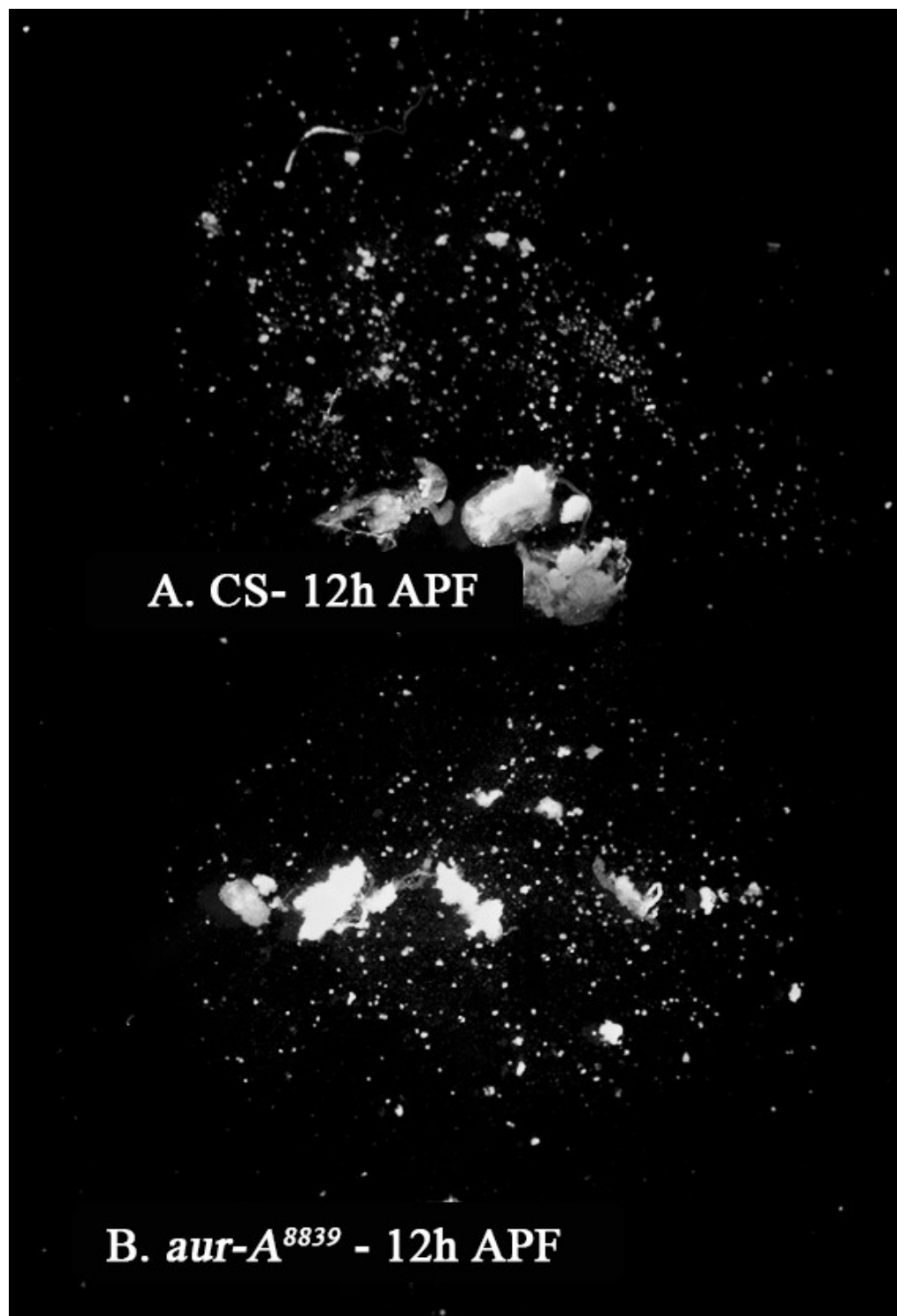


Figure 12. Fat body remodeling of mutant samples compared to wild type at 12h APF. A shows the fat body remodeling of the CS while B shows the fat body remodeling of *aur-A*⁸⁸³⁹. Images taken with the stereoscope and edited by Photoshop.

At 14h APF, in the first mutant sample, a few fat bodies were remodeled. Clusters were observed. In the second mutant sample, the majority of larval fat bodies were individual sphere-like cells. There was no significant difference observed in the degree of remodeling between the second mutant line and wild type (Figure 13).

Possible developmental delay was observed in most samples of *aur-A*⁸⁸³⁹ during dissection, which looked similar to Figure 9.

Not all samples imaged were included in this paper for *aur-A*⁸⁸³⁹.

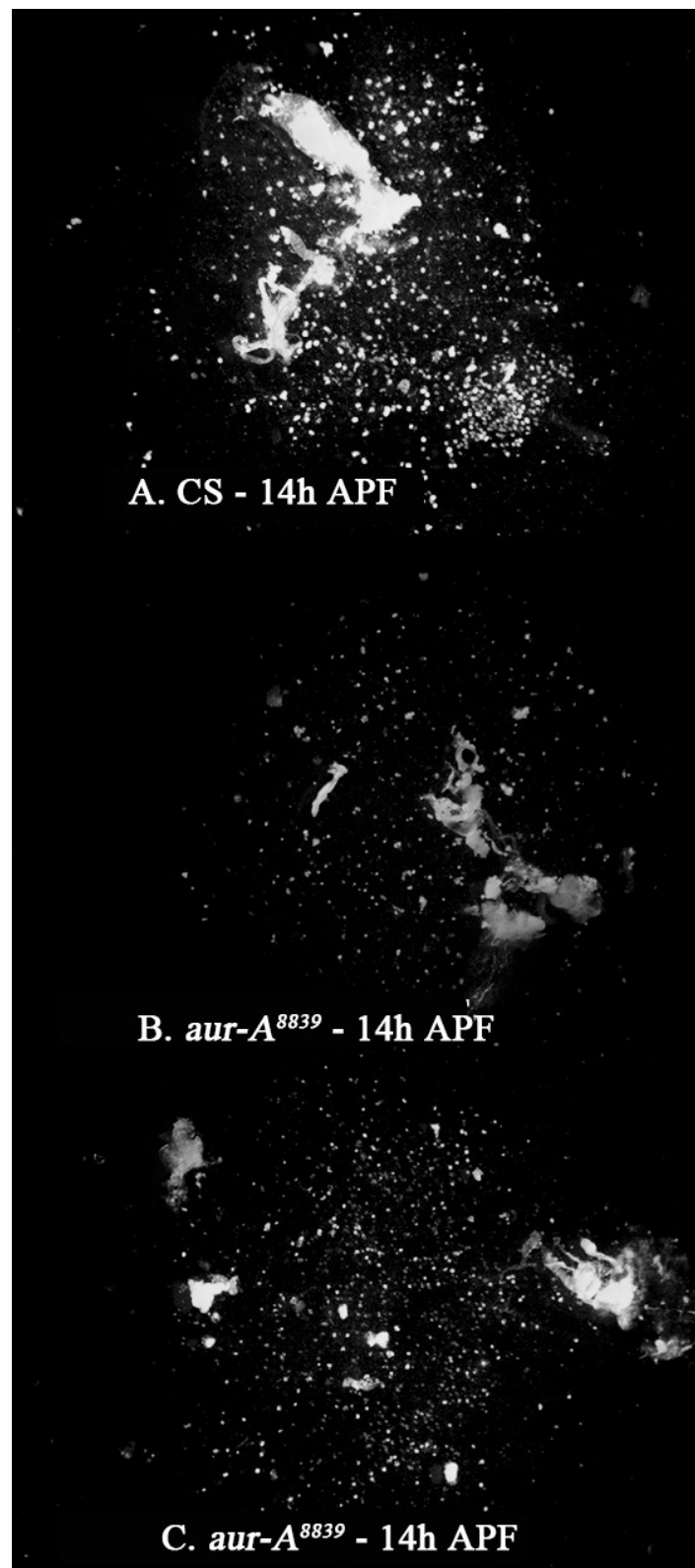


Figure 13. Fat body remodeling of mutant samples compared to wild type at 14h APF. A shows the fat body remodeling of the CS while B and C show the fat body remodeling of *aur-A*⁸⁸³⁹. Images taken with the stereoscope and edited by Photoshop.

Abnormal FBR feature of 15241

At 11h APF, clusters of fat bodies were observed. There was no significant difference observed in the degree of remodeling between the mutant line and wild type (Figure 14).

At 12h APF, in the first mutant sample, little individual fat bodies were observed, while in the second mutant sample, the majority of fat bodies were remodeled (Figure 15). Compared to wild type (Figure 12-A), there was no significant difference observed in the degree of remodeling.

At 14h APF, the majority of the fat bodies were individual sphere-like cells. There was no significant difference observed in the status of remodeling between the mutant line and wild type (Figure 16).

Possible developmental delay was observed in only one sample of 15241 during dissection, which looked similar to Figure 9. No sign of developmental delay was observed in the rest of the samples.

Not all samples imaged were included in this paper for 15241.

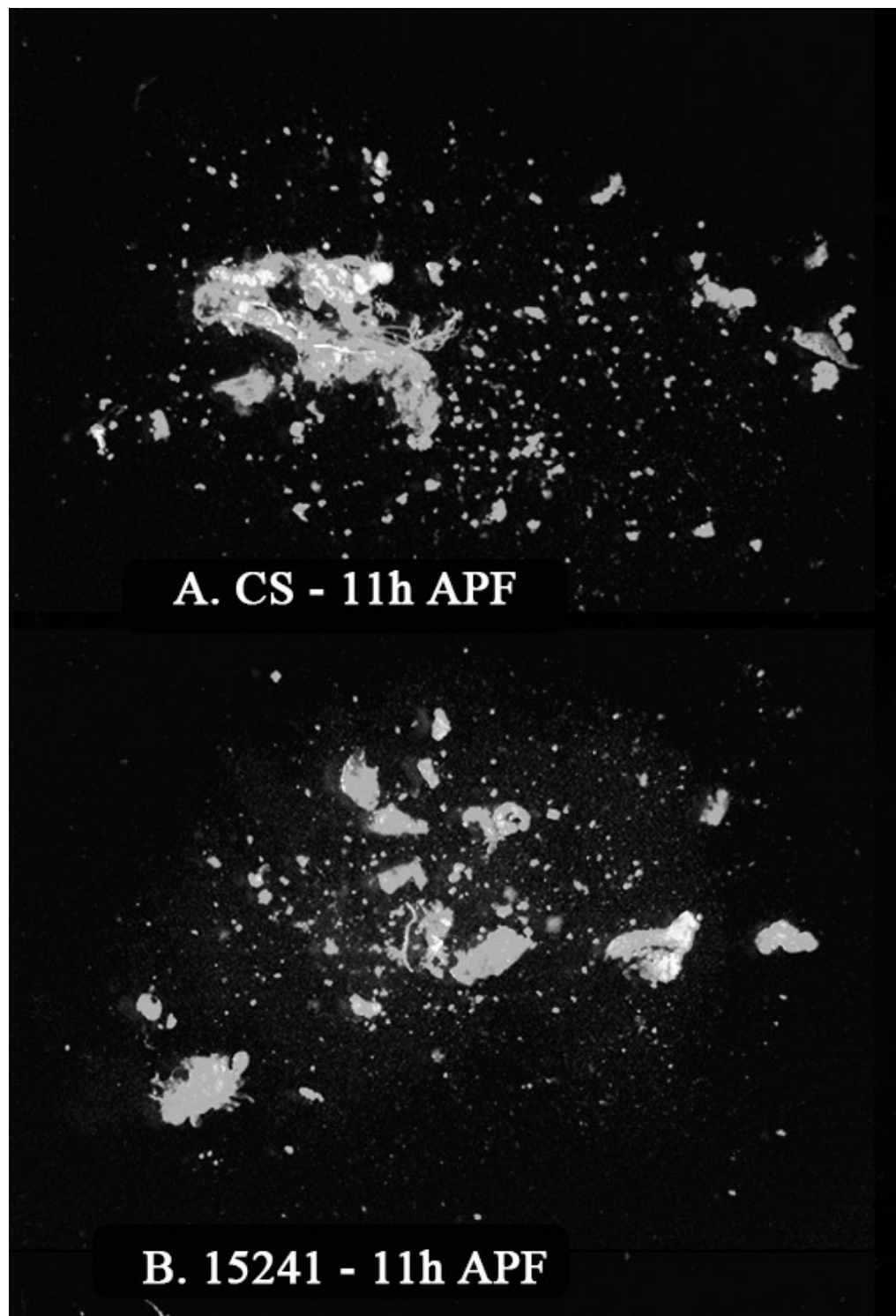


Figure 14. Fat body remodeling of mutant samples compared to wild type at 11h APF. A shows the fat body remodeling of the CS while B shows the fat body remodeling of 15241. Images taken with the stereoscope and edited by Photoshop.

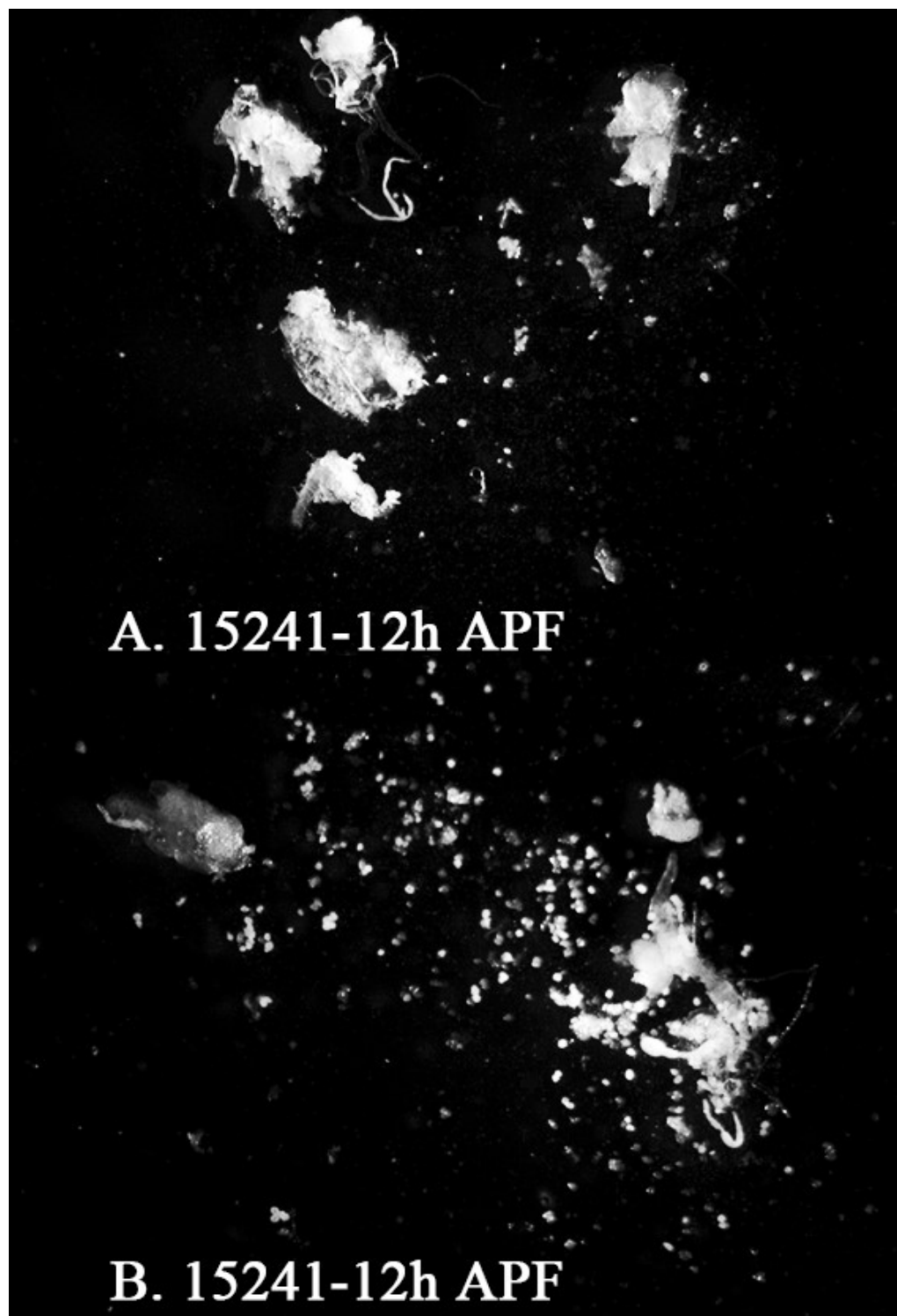


Figure 15. Fat body remodeling of mutant samples compared to wild type at 12h APF. A and B show the fat body remodeling of 15241. Images taken with the stereoscope and edited by Photoshop.

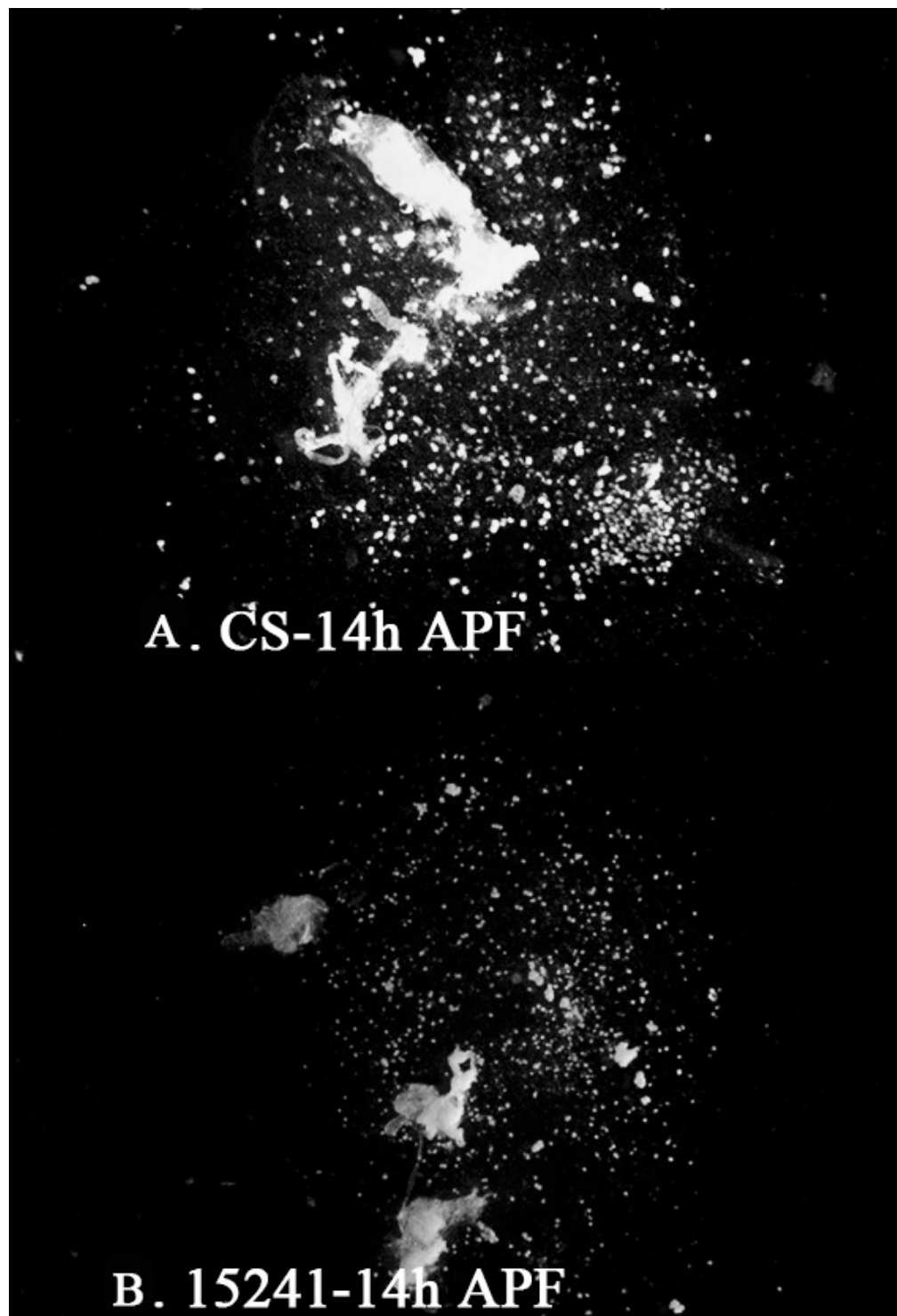


Figure 16. Fat body remodeling of mutant samples compared to wild type at 14h APF. A shows the fat body remodeling of wild type, while B shows the fat body remodeling of 15241. Images taken with the stereoscope and edited by Photoshop.

Varieties in larval fat bodies' colors after remodeling

Two types of remodeled larval fat bodies were observed in *aur-A*¹⁴⁶⁴¹, *aur-A*⁸⁸³⁹, 15241 and the CS, showing the common existence of the following feature: one type of remodeled fat bodies were whitish, and the other type of remodeled fat bodies were clear. The two types of remodeled fat bodies were observed at multiple time points APF, and no trend was observed between their relative amounts and the age of the individual (Figure 17). Some clusters of fat bodies were composed of mostly whitish fat bodies, but not enough data was collected to confirm this observation.

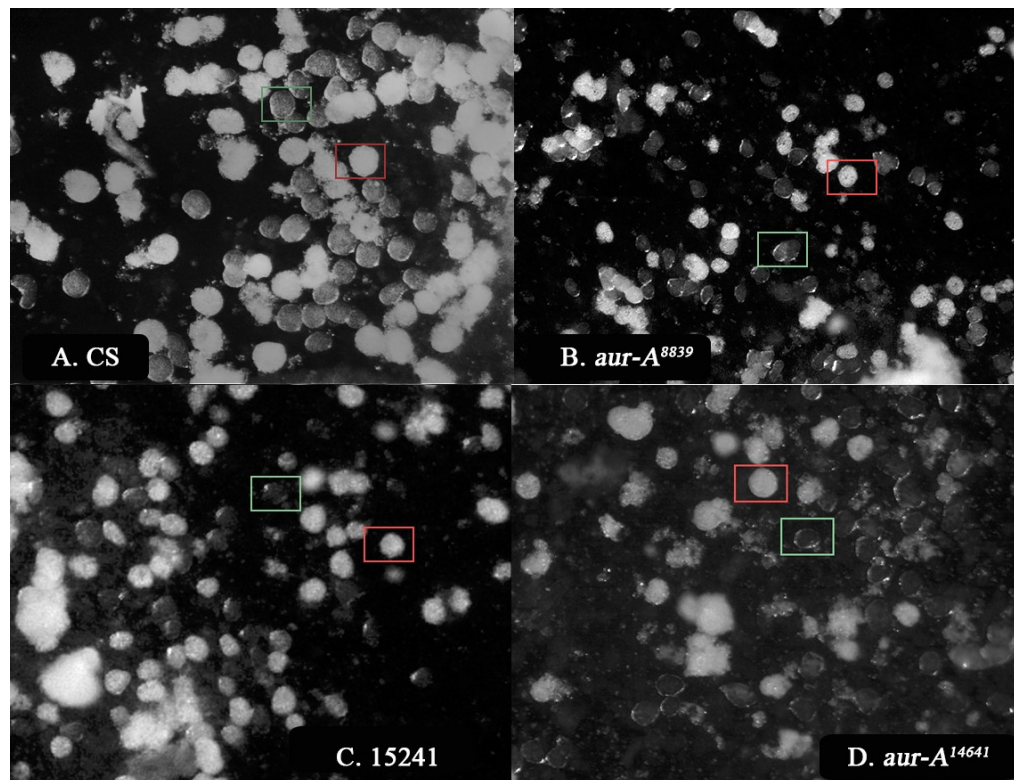


Figure 17. The clear remodeled fat bodies and whitish remodeled fat bodies in different mutant lines and wild type. A shows remodeled fat bodies of wild type CS; B shows remodeled fat bodies of mutant *aur-A*⁸⁸³⁹; C shows remodeled fat bodies of mutant 15241; D shows remodeled fat bodies of mutant *aur-A*¹⁴⁶⁴¹. An example of clear remodeled fat bodies in each line was marked by green rectangles, while an example of whitish remodeled fat bodies in each line was marked by red rectangles. Images taken with the stereoscope and edited by Photoshop.

Staining remodeled fat bodies from wild type w^{1118}

Six individuals from wild type w^{1118} were dissected at 13h APF, and their remodeled fat bodies were collected for staining. Figure 18 and 19 showed that one remodeled fat body was composed of multiple sphere-like lipid droplets of various sizes (red), and nucleus were surrounded in the middle (blue). Some fat bodies showed less lipid droplets surrounding the nucleus, which were shown with white squares in Figure 19. They could be broken fat bodies, where lipid droplets were lost during staining. There were floating lipid droplets in the background of Figure 18 and 19, which might also come from broken fat bodies during staining.

During staining, it was found that in PBS buffer with 1% BSA, fat bodies might show different densities. When the imaging spacer was filled with the buffer solution to create a convex surface, some fat bodies were floating on the top of the surface, while other fat bodies were sunk on the bottom of the slide.

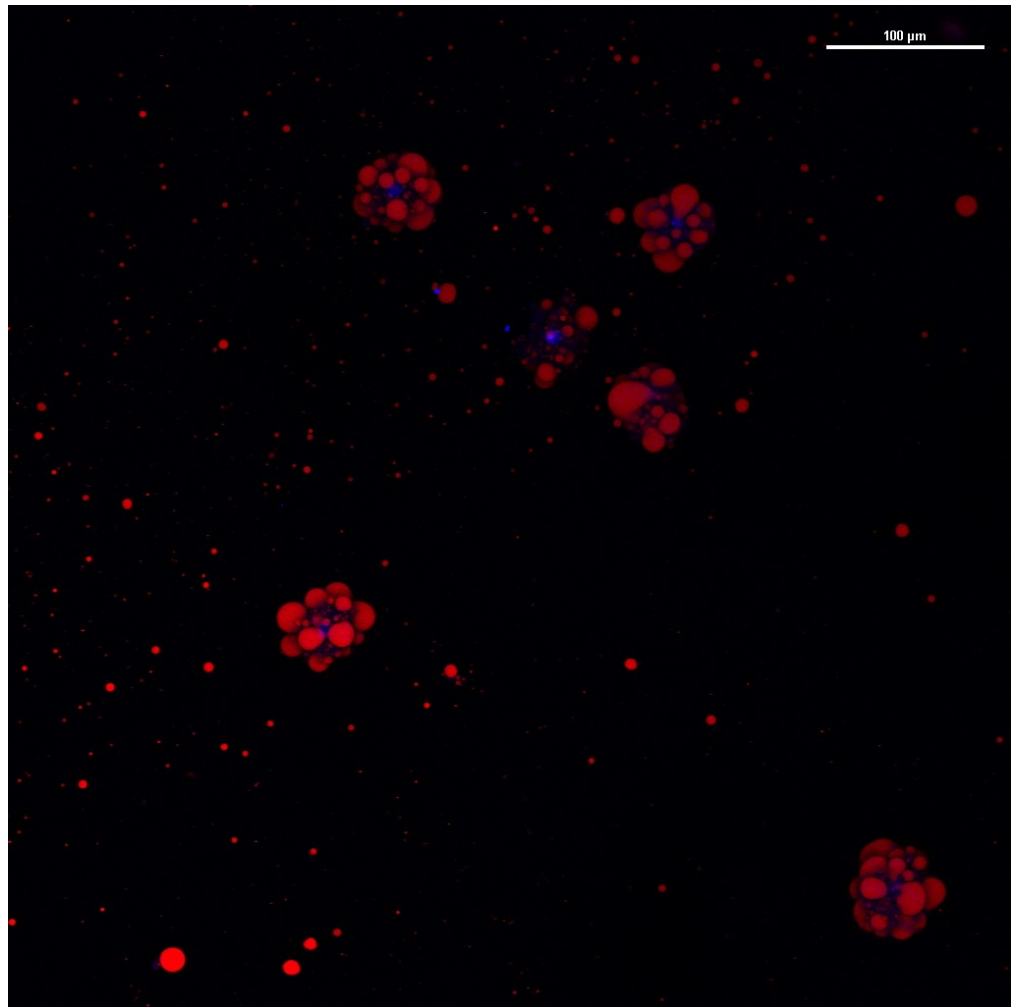


Figure 18. Remodeled larval fat bodies under the 30x confocal microscope from wild type w^{1118} . The fat bodies were collected from 6 individuals at 13h APF. The lipid droplets were stained by Nile Red, showing fluorescence in red, and the nucleus were stained by DAPI, showing fluorescence in blue.

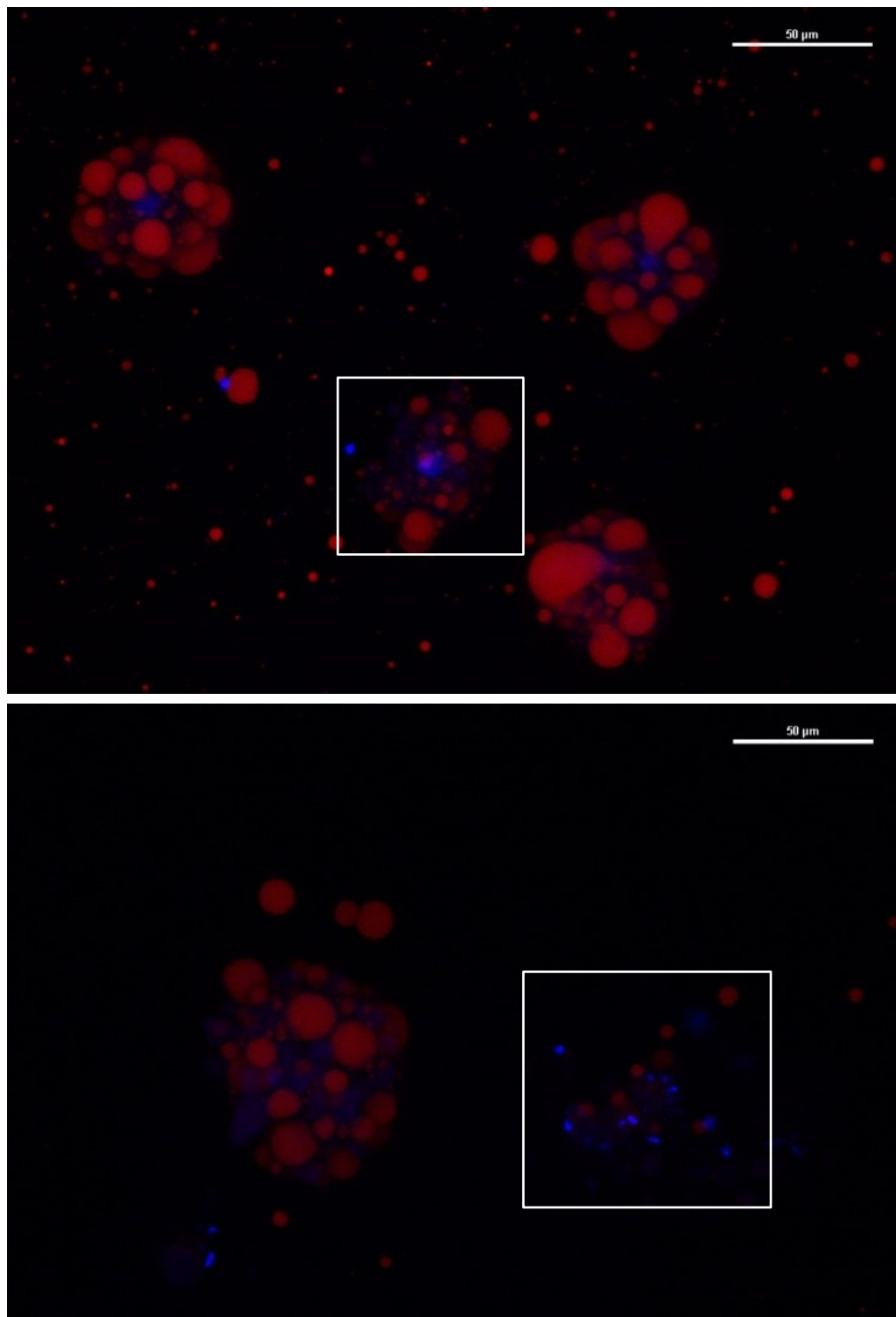


Figure 19. Remodeled fat bodies under the 40x confocal microscope from wild type w^{1118} . The fat bodies were collected from 6 individuals at 13h APF. The lipid droplets were stained by Nile Red, showing fluorescence in red, and the nucleus were stained by DAPI, showing fluorescence in blue. Possible broken fat bodies are marked with white squares (continuing on the next page).

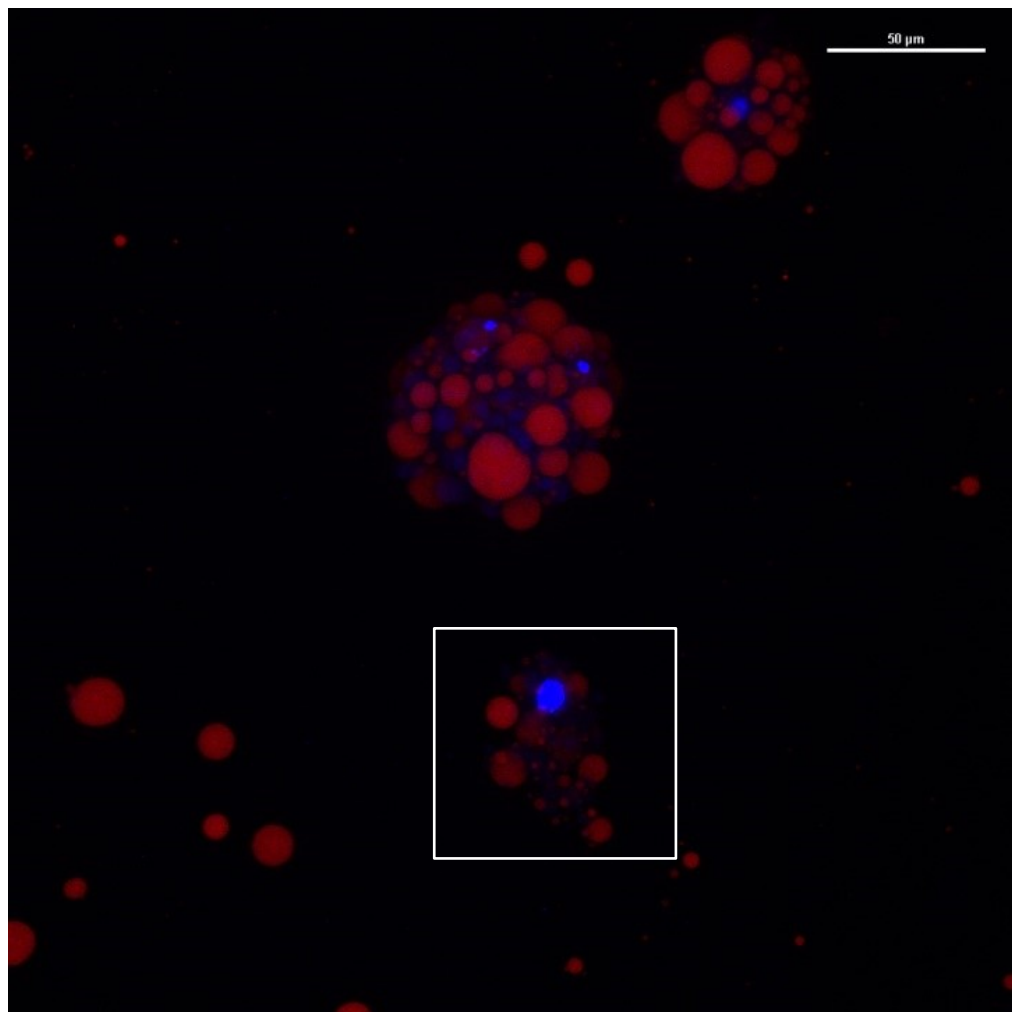


Figure 19. Remodeled fat bodies under the 40x confocal microscope from wild type w^{1118} . The fat bodies were collected from 6 individuals at 13h APF. The lipid droplets were stained by Nile Red, showing fluorescence in red, and the nucleus were stained by DAPI, showing fluorescence in blue. Possible broken fat bodies are marked with white squares.

DISCUSSION

Penetrance is the likelihood of a phenotype to show up when an individual carries the corresponding genotype. Complete penetrance happens when phenotypes are shown in all individuals carrying the genotype. My results showed that, although in all three mutant lines, there were individuals found to bear the abnormal FBR phenotype, it was obvious that this phenotype did not happen as often as its genotype. Thus, I concluded that the three mutant lines were incompletely penetrant for the abnormal FBR phenotype. Incomplete penetrance means that while some mutant individuals show failure or abnormality in larval fat body remodeling, others do not. Incomplete penetrance is commonly seen in genetic mutations and could be measured quantitatively, where we divide the number of individuals showing the phenotype by the number of individuals carrying the genotype (Miko, 2008). In case of my research, a larger sample size will be necessary in order to measure the exact penetrance in the three mutant lines, but based on the data I got so far, the three mutant lines should have low penetrance under our experimental conditions. Because of the complexity of pathways during gene transcription and protein expression, there could be many explanations on why incomplete penetrance happens. One possibility could be related to how other genes act as regulators to influence our gene of interest (gene background). To exclude the effect of gene background, we could choose model organisms with

a low variability in genomes. Another possibility is the difference in expression levels. To exclude its effect, we could develop a method to measure the expression of our gene of interest. Overall, it will be difficult to study why and how incomplete penetrance happens (Miko, 2008).

For any further experiment, I would suggest that we try varying experimental conditions such as temperatures and dietary. Since clusters of fat bodies also showed up in wild type, it is possible that there were environmental factors leading to partial failure or delay of FBR. Varying experimental conditions should be the easiest way to try out in order to increase the penetrance, and after that, we could make the decision on whether we will switch to mutant lines with more severe phenotypes.

Expressivity is another term related to abnormal FBR phenotype results of my research. It's the severity of a phenotype seen in an individual with a specific mutant genotype, and individuals carrying the same genotype could show different degrees of the corresponding phenotype. While I predicted that the variability in expressivity should exist in my mutant lines, I didn't mention it in the result section because either qualitative scale or quantitative method was used in my experiments. To obtain better data in expressivity, I will suggest that we develop a scale to categorize different degrees of FBR or a quantitative method to measure the degree of FBR in an individual. One possible quantitative method is to calculate the % dissociation by estimating

the size of remodeled fat bodies under the stereoscope (Jia et al. 2014). These solutions should also improve our judgments on the existence of incomplete penetrance.

Possible developmental delay was observed in most of the individuals from the two *aur-A* mutant lines during head eversion, while little developmental delay was observed in 15241. In all three mutant lines, the *Tubby* larvae (heterozygotes or non-mutant individuals with shorter and fatter appearance) were observed to enter the prepupa stage (being out of food and forming the pupal case) much faster than the mutant homozygotes (with normal appearance). As *Tubby* individuals entered the prepupa stage, little or no samples of mutant homozygotes were observed to enter the 3rd instar stage. Due to the lack of data and quantitative method, I cannot give any conclusion on developmental delay of the three mutant lines, either during head eversion or during the larva stage. This is a direction that any further research could focus on.

Whitish and clear fat bodies were observed in *aur-A*¹⁴⁶⁴¹, *aur-A*⁸⁸³⁹, 15241 and CS (Figure 17). No difference was observed between mutant lines. No trend was observed between their relative amounts and their ages. Although I didn't find any discussion about this phenomenon in literatures, there were images from previous research showing the two types of fat bodies (Figure 20).

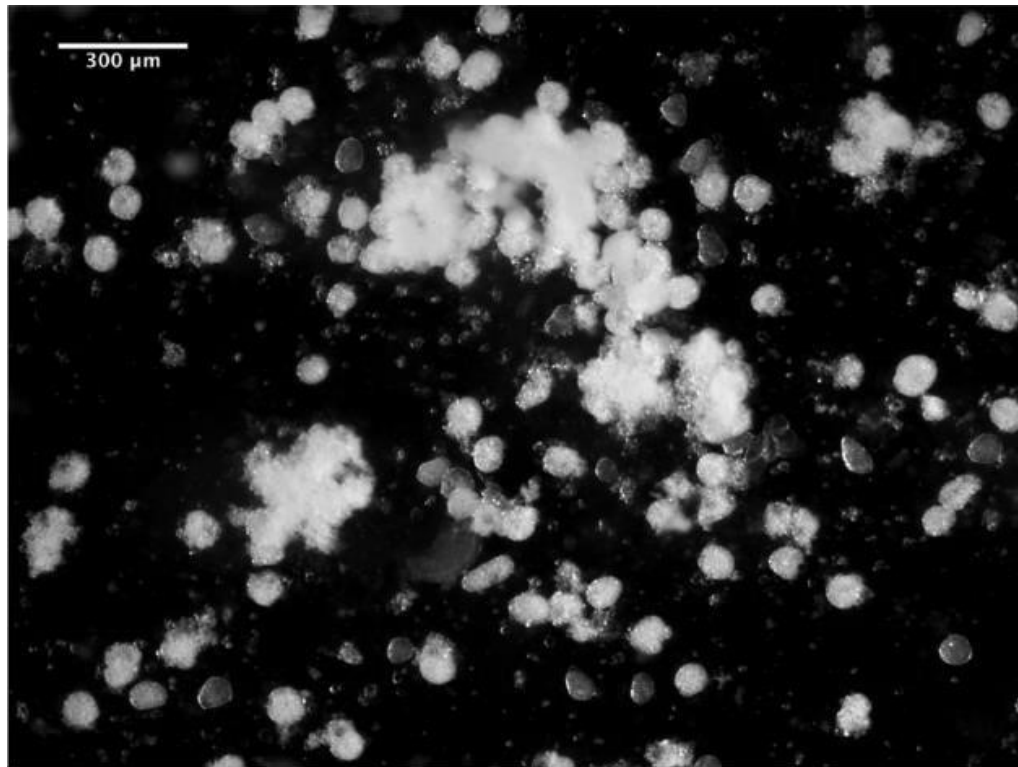


Figure 20. Progeny dissection of the *I(3)LL-11075: L 04 PA x I(3)LL-2310: L 04 PA* mutant cross at 14 hours APF. Categorized as partial remodeling. Whitish and clear fat bodies could be seen in this image (Arshinoff, 2017).

Fat bodies contain energy storage molecules in the form of lipids, glycogen and proteins. Among the three, lipid droplets are the major storage molecules, representing more than 50% of the dry weight (Arrese, 2010). Therefore, I hypothesize that the whitish fat bodies bear a higher amount of lipid storage inside, while the clear fat bodies bear a lower amount of lipid storage inside. To test this hypothesis, the first step is to visualize the lipid storage in remodeled larval fat bodies, and I've completed one successful trial in staining remodeled fat bodies using Nile Red and DAPI (Figure 18 and 19). I think my method is valid in testing my hypothesis, but the efficiency needs further improvement. As mentioned in the result section, it is possible that some fat bodies were broken during staining, forming abnormal-looking fat bodies and floating lipid droplets in the background (Figure 19). While I've used multiple individuals from *w¹¹¹⁸* to collect remodeled fat bodies, their densities were still low under the confocal microscope. Thus, it's necessary to improve my method in order to reduce the amount of lost fat bodies during staining.

Once a sufficient staining method is developed, we should stain identified whitish or clear fat bodies in order to test any difference in their lipid storage. We will have to work out how the two types of fat bodies can be separated from each other before staining. Based on my experience of pupae dissection, it's possible to group different fat bodies manually with pipettes or tweezers.

If my hypothesis on the two types of fat bodies is supported by future data, it will be possible to see how lipid storage changes at different time points APF in the mutant lines compared to wild type. If whitish fat bodies do bear more lipid storage, less of them should be observed as the pupa getting closed to the adult stage (completion of metamorphosis), since much energy has been used. If clear fat bodies do bear less lipid storage, less of them should be observed at the beginning of metamorphosis, since little energy has been used. Another interesting topic to explore will be the distribution of lipid storage before, during and after metamorphosis, which might provide evidence on the timeline of metamorphosis in different parts of the organism.

In conclusion, the three mutant lines, *aur-A*¹⁴⁶⁴¹, *aur-A*⁸⁸³⁹, and 15241 were found to be incompletely penetrant. Two types of remodeled larval fat bodies, whitish fat bodies and clear fat bodies were observed in both mutant lines and wild type. Further research should continue on testing lipid storage of fat bodies by lipid droplets staining, which might give insights into how fat body cells regulate their nutrient.

LITERATURE CITED

- Arrese, Estela L., and Jose L. Soulages. 2010. Insect fat body: energy, metabolism, and regulation. *Annual Review of Entomology* 55 : 207-25.
- Bond, Nichole D., Archana Nelliott, Marsha K. Bernardo, Melanie A. Ayerh, Kathryn A. Gorski, Deborah K. Hoshizaki, and Craig T. Woodard. 2011a. β FTZ-F1 and matrix metalloproteinase 2 are required for fat-body remodeling in *Drosophila*. *Developmental Biology* 360 (2): 286-96.
- Bond, Nichole D., Archana Nelliott, Marsha K. Bernardo, Melanie A. Ayerh, Kathryn A. Gorski, Deborah K. Hoshizaki, and Craig T. Woodard. 2011b. ssFTZ-F1 and matrix metalloproteinase 2 are required for fat-body remodeling in *Drosophila*. *Developmental Biology* 360 (2): 286-96.
- Chyb, Sylwester, and Nicolas Gompel. 2013. *Atlas of Drosophila morphology: Wild-type and classical mutants*. Academic Press.
- Cox, Thomas R., and Janine T. Erler. 2011. Remodeling and homeostasis of the extracellular matrix: Implications for fibrotic diseases and cancer. *Disease Models & Mechanisms* 4 (2): 165-78.
- Danielle Arshinoff. 2017. The role of aur-A in *Drosophila melanogaster* fat body remodeling. Mount Holyoke College (Senior honors thesis).
- DANØ, KELD, JOHN RØMER, BOYE S. NIELSEN, SIGNE BJØRN, CHARLES PYKE, JØRGEN RYGAARD, and LEIF R. LUND. 1999. Cancer invasion and tissue remodeling-cooperation of protease systems and cell types. *Apmis* 107 (1-6): 120-7.
- Franz, Anna, Will Wood, and Paul Martin. 2018. Fat body cells are motile and actively migrate to wounds to drive repair and prevent infection. *Developmental Cell* 44 (4): 460,470. e3.
- Gausz, J., H. Gyurkovics, G. Bencze, AAM Awad, J. J. Holden, and D. Ish-Horowicz. 1981. Genetic characterization of the region between 86F1, 2 and 87B15 on chromosome 3 of *Drosophila melanogaster*. *Genetics* 98 (4): 775-89.
- Greenspan, Phillip, Eugene P. Mayer, and Stanley D. Fowler. 1985. Nile red: A selective fluorescent stain for intracellular lipid droplets. *The Journal of Cell Biology* 100 (3): 965-73.
- Grönke, Sebastian, Mathias Beller, Sonja Fellert, Hariharasubramanian Ramakrishnan, Herbert Jäckle, and Ronald P. Kühnlein. 2003. Control of

fat storage by a *Drosophila* PAT domain protein. *Current Biology* 13 (7): 603-6.

Jennings, Barbara H. 2011. *Drosophila – a versatile model in biology & medicine*. Vol. 14.

Jia, Qiangqiang, Yang Liu, Hanhan Liu, and Sheng Li. 2014. Mmp1 and Mmp2 cooperatively induce *Drosophila* fat body cell dissociation with distinct roles. *Scientific Reports* 4 (1): 7535.

Johnsen, Morten, Leif R. Lund, John Rømer, Kasper Almholt, and Keld Danø. 1998. *Cancer invasion and tissue remodeling: Common themes in proteolytic matrix degradation*. Vol. 10.

Kamoshida, Yuki, Sally Fujiyama-Nakamura, Shuhei Kimura, Eriko Suzuki, Jinseon Lim, Yumi Shiozaki-Sato, Shigeaki Kato, and Ken-ichi Takeyama. 2012. Ecdysone receptor (EcR) suppresses lipid accumulation in the *Drosophila* fat body via transcription control. *Biochemical and Biophysical Research Communications* 421 (2): 203-7.

Kapuscinski, Jan. 1995. DAPI: a DNA-specific fluorescent probe. *Biotechnic & Histochemistry* 70 (5): 220-33.

Li, Sheng, Xiaoqiang Yu, and Qili Feng. 2019. Fat body biology in the last decade. *Annual Review of Entomology* 64 (1): 315-33.

Lu, Pengfei, Ken Takai, Valerie M. Weaver, and Zena Werb. 2011. Extracellular matrix degradation and remodeling in development and disease. *Cold Spring Harbor Perspectives in Biology* 3 (12): a005058.

Miko, Ilona. 2008. Phenotype variability: penetrance and expressivity. *Nature Education* 1 (1): 137.

Moon, Woongjoon, and Fumio Matsuzaki. 2013. Aurora A kinase negatively regulates rho-kinase by phosphorylation in vivo. *Biochemical and Biophysical Research Communications* 435 (4): 610-5.

Nelliot, Archana, Nichole Bond, and Deborah K. Hoshizaki. 2006. Fat body remodeling in *Drosophila melanogaster*. *Genesis* 44 (8): 396-400.

Okamura, Tomoo, Hideyuki Shimizu, Tomoko Nagao, Ryu Ueda, and Shunsuke Ishii. 2007. ATF-2 regulates fat metabolism in *Drosophila*. *Molecular Biology of the Cell* 18 (4): 1519-29.

Oudin, Madeleine J., Oliver Jonas, Tatsiana Kosciuk, Liliane C. Broye, Bruna C. Guido, Jeff Wyckoff, Daisy Riquelme, John M. Lamar, Sreeja B. Asokan, and Charlie Whittaker. 2016. Tumor cell-driven extracellular

- matrix remodeling drives haptotaxis during metastatic progression. *Cancer Discovery* 6 (5): 516-31.
- Riddiford, Lynn M., and James W. Truman. 1993. Hormone receptors and the regulation of insect metamorphosis. *American Zoologist* 33 (3): 340-7.
- Robertson, Charles William. 1936. The metamorphosis of *Drosophila melanogaster*, including an accurately timed account of the principal morphological changes. *Journal of Morphology* 59 (2): 351-99.
- Ruaud, Anne-Françoise, Geanette Lam, and Carl S. Thummel. 2010. The *Drosophila* nuclear receptors DHR3 and FTZ-F1 control overlapping developmental responses in late embryos. *Development* 137 (1): 123-31.
- Semwogerere, Denis, and Eric R. Weeks. 2005. Confocal microscopy. *Encyclopedia of Biomaterials and Biomedical Engineering* 23 : 1-10.
- Thummel, Carl S. 1996. Flies on steroids -- *Drosophila* metamorphosis and the mechanisms of steroid hormone action. *Trends in Genetics* 12 (8): 306-10.
- Tiede, Svenja L., Matthias Wassenberg, Katrin Christ, Ralph T. Schermuly, Werner Seeger, Friedrich Grimminger, Hossein Ardeschir Ghofrani, and Henning Gall. 2016. Biomarkers of tissue remodeling predict survival in patients with pulmonary hypertension. *International Journal of Cardiology* 223 : 821-6.
- Tyler, Mary S. 1994. *Developmental biology: A guide for experimental study*.
- Uswa Iqbal. 2018. Mapping genes involved in *Drosophila melanogaster* larval fat body remodeling. Mount Holyoke College(Senior Honors Thesis).
- Weigmann, Katrin, Robert Klapper, Thomas Strasser, Christof Rickert, Gerd Technau, Herbert Jäckle, Wilfried Janning, and Christian Klömbt. 2003. FlyMove -- a new way to look at development of *Drosophila*. *Trends in Genetics* 19 (6): 310-1.
- White, J. G., W. B. Amos, and M. Fordham. 1987. An evaluation of confocal versus conventional imaging of biological structures by fluorescence light microscopy. *The Journal of Cell Biology* 105 (1): 41-8.